HEINRICH=HERTZ=INSTITUT FÜR SCHWINGUNGSFORSCHUNG
BERLIN=CHARLOTTENBURG

Technischer Bericht Nr. 145

Messung des vollständigen elektromagnetischen
Feldes von Längstwellensendern

Measurement of the complete electromagnetic
field of VLF transmitters

von

Dr. rer. nat. Joachim Frisius / Ing. Günter Heydt / Ing. grad. Rainer Raupach

Berlin

1971

Measurement of the complete electromagnetic field of VLF transmitters

Summary:

The actions of the new VLF routine recording equipment of the H.H.I. are des-
cribed. The previous records of field strength amplitude and phase on 16 kHz
have been extended by including observations on 60 kHz and observations of para-
meters characterizing the elliptizity of the received horizontal magnetic vector.
In this way the transversal electric component of the field caused by the anisotro-
pic ionospheric reflection can be separated from the transversal magnetic com-
ponent. Examples of monthly observation reviews are given.

Messung des vollständigen elektromagnetischen Feldes von Längstwellensendern

Zusammenfassung:

Die Wirkungsweise des neuen Längstwellen-Meßplatzes des H.H.I. wird beschrie-
ben. Die Registrierungen von Feldstärke-Amplitude und Phase auf 16 kHz werden
erweitert durch Einbeziehung einer weiteren Meßfrequenz (60 kHz) und durch Be-
obachtung der Elliptizität des horizontalen magnetischen Vektors. Der Zusammen-
hang zwischen den gemessenen Elliptizitäts-Parametern und den TM und TE-Kom-
ponenten des empfangenen magnetischen Vektors wird dargestellt. Beispiele monat-
licher Übersichten über Registrierungen werden mitgeteilt.

Heinrich-Hertz-Institut für Schwingungsforschung
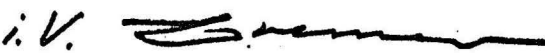
Die Bearbeiter

(Dr. rer. nat. J. Frisius)   (Ing. G. Heydt)   (Ing. grad. R. Raupach)

Der Abteilungsleiter   Der Institutsdirektor

                                        i. V.

(Prof. Dr. -Ing. F. W. Gundlach)   (Prof. Dr. -phil. P. Matthieu)

Berlin-Charlottenburg, d. 12. Oktober 1971

Measurement of the complete electromagnetic field of VLF transmitters

1. Introduction

The Abteilung Hochfrequenztechnik of the Heinrich-Hertz-Institut, Berlin-Charlottenburg, has carried out contineous observations of the field strength amplitude and -phase of the transmitter GBR (16 kHz) since 1958 (Eppen and Heydt, 1959, Volland 1960). According to the state of technique available at that time, the observations were stored by ink recorders providing a lot of registration paper that fills the archives of the H.H.I. up to now. Only samples of this material have been published, playing the role of illustrating theoretical work on VLF propagation. For steady systematic evaluation, e. g. determination of the diurnal variations of the reflection height and reflection attenuation (Volland, 1968, Frisius, 1966, 1970), neither the personnel nor the necessary technical auxiliary means were available. The regular data exchange has therefore been restricted up to day to regular messages of the solar flare effects that could be read off from the records. (Ionosphärenberichte des Deutschen Wetterdienstes und der Arbeitsgemeinschaft Ionosphäre). In this way, the requirements for steady exchange of geophysical data are not very well satisfied. Therefore, the development of a new VLF data system has been initiated in 1967. To meet the interests of geophysicists and meteorologists we have attempted to find a way of data presenting that

a) demonstrates the influence of the sun's zenith angle on the observed parameters at first sight,

b) reduces the information abundance of normal ink records to such a degree that the diurnal field variations are sufficiently described by a set of numerical data appropriate for regular exchange and automatical data processing.

Theoretical studies (Volland , 1968) indicate that the electromagnetic field excited by a VLF transmitter in the earth-ionosphere wave guide provides more information on the ionospheric reflection than the usual records of one or two field quantities (e.g. amplitude and/or phase of the vertical electric component). Additional recording of other components may be expected to permit the determination of the ionospheric conversion coefficients.

It happened that in course of a preceding H.H.I.-Project, the development of the Atmospherics-Analyzer (Heydt, 1967), simple analog methods for direction finding and measuring the ellipticity of the horizontal magnetic field were developed. These methods have been adapted to extend the former field strength records to a "full wave" measurement of the received electromagnetic field. Details of the technique will be published by a technical report (Raupach and Heydt, in print). Here we restrict ourselves to describe the quantities observed by the H.H.I., and their graphical presentation, that is planned to be published regularly over a period of two or three years, say.

2. Description of the observed parameters

All measurements are carried out by means of an antenna system consisting in two crossed loops (area = 1 m^2, number of turns = 24) and a vertical whip (length 4.5 m), mounted on the roof of the institute (elevation over ground ca. 45 m). The measured quantities are
1. Amplitude E of the vertical component of the electric field vector,
2. Phase Φ_E of the same component, measured relatively to the institute's frequency normal (Raupach, 1970),

These measurements continue the preceding observations of the H.H.I. and are not further considered in this report.

3. Deviation φ of the apparent bearing angle Ψ from the direction of the great circle connecting the receiver's position and GBR,

4. Amplitude H of the magnetic component parallel to the ground and perpendicular to the apparent bearing direction,

5. Phase $\bar{\Phi}_H$ of the same component, measured relatively to the institute's frequency normal,

6. Ratio between the smaller and the larger principal axis of the oscillation ellipse of the horizontal magnetic vector (HPR = $\underline{H}$ - polarization - $\underline{r}$atio).

The phase measurements are carried out on 16 kHz only (GBR), all other measurements on 16 kHz and 60 kHz (MSF). Before considering the observed quantities in more detail we show an example of recordings taken in the summer 1971. The fluctuations of the field strength amplitude and phase during night, well known from the previous observations, are accompanied by variations of the apparent angle of arrival and of the magnetic ellipticity ratio, especially on 60 kHz. During daytime, no magnetic ellipse can be observed. (see Fig. 1).

The physical discussion of these phenomena must be postponed to later work. In the following section the relations between the observed parameters and the transversal magnetic (TM) and the transversal electric (TE) component of the magnetic vector will be compiled.

3. Analysis of the magnetic field

For simplification, we neglect the earth's curvature and choose the transmitter's position as the origin of a cartesian coordinate system X and Y. The positive Y-axis points to north, the X-axis to East. The angle between the X-axis and the radius vector showing from the transmitter to the receiver is $\emptyset$. The "true bearing angle" Ψ_o is the angle between the positive Y-axis (= geographic North) and the
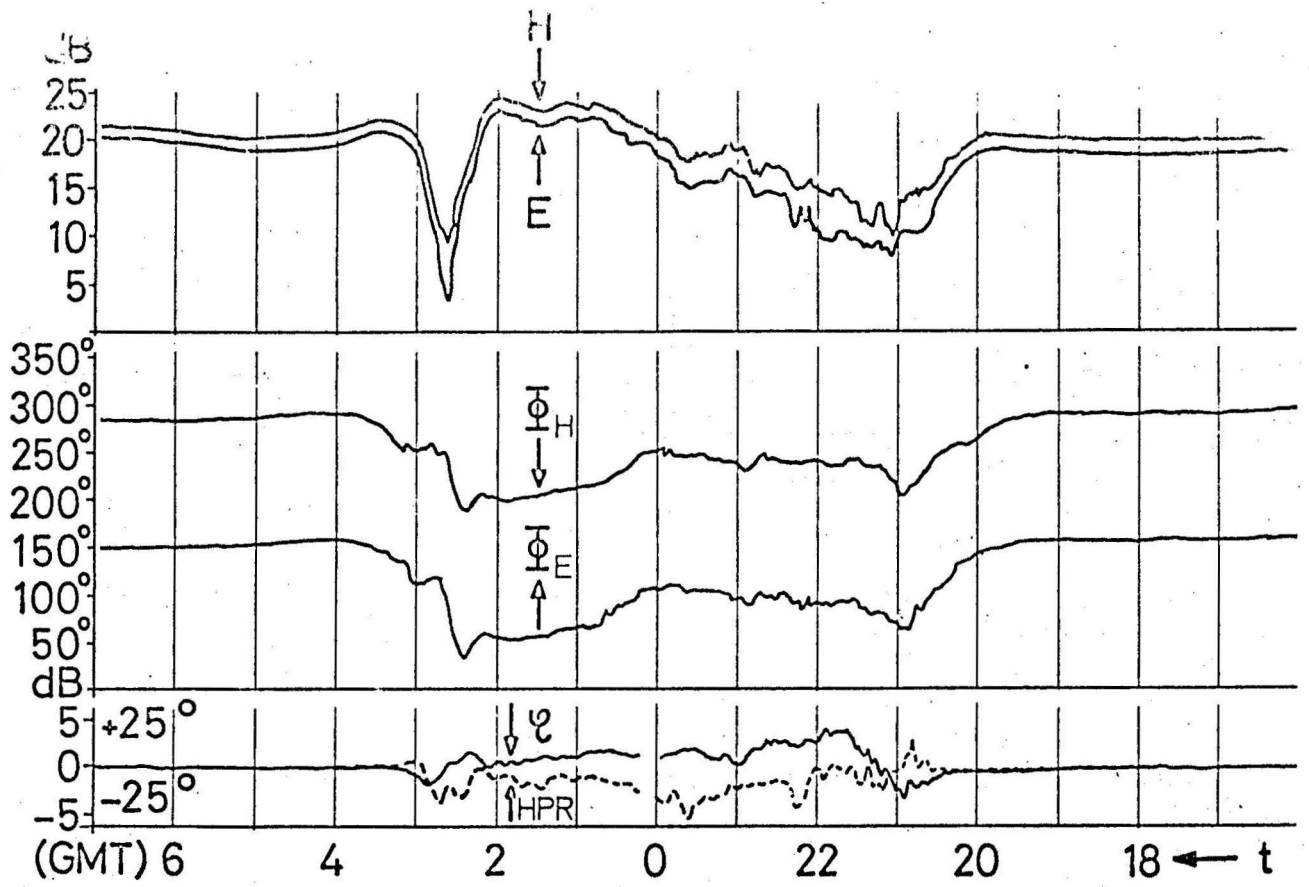
16 kHz   Berlin   20.7.1971
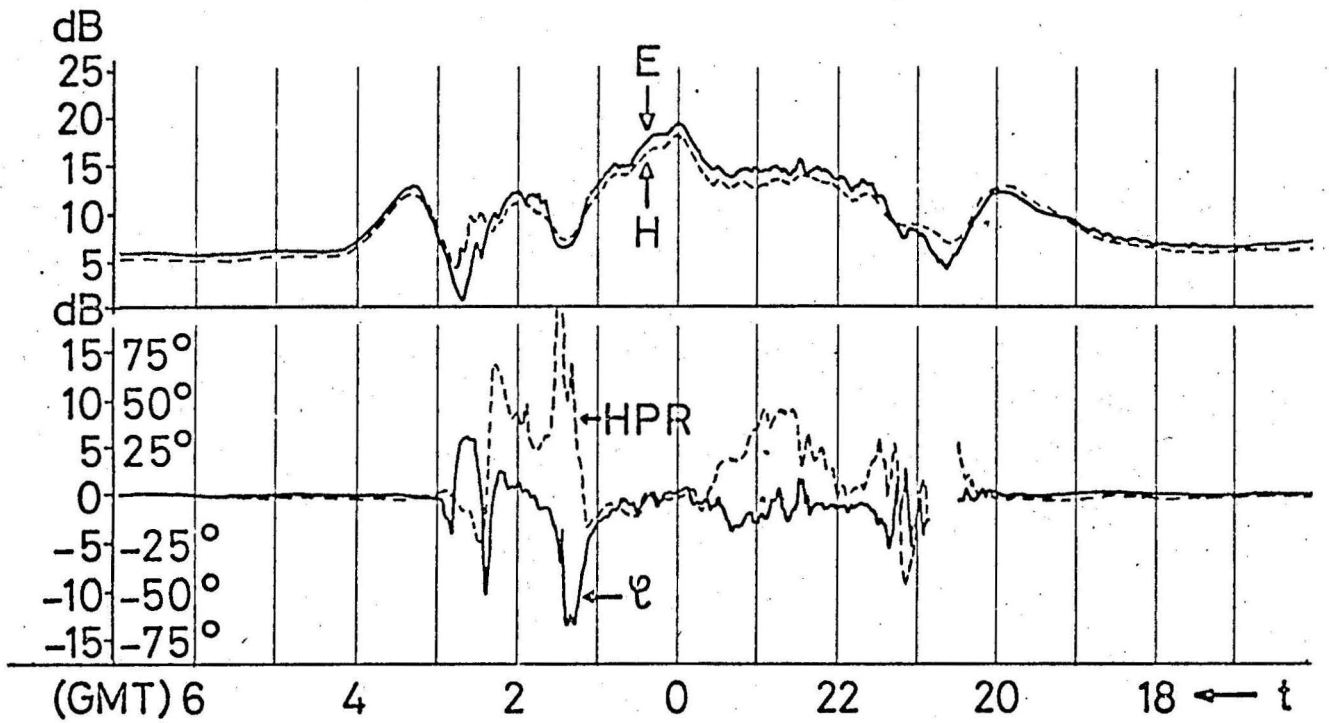
60 kHz   Berlin   20.7.1971

Fig. 1: Examples of Records

radius vector showing in opposite direction from the recei-
ver to the transmitter: (see Fig. 2)

$$\Psi_0 = (\frac{\pi}{2} - \phi) + \pi \tag{1}$$

In interest of generality of the following considerations, we
assume the receiver's loop antennas to be oriented in such a
way that their normals coincide with the geographic West-East
and North-South directions (N.B.: We call briefly X- or Y-
antenna that loop the normal of which coincides with the +X
or +Y axis respectively).

The receiver's position is chosen to be the origin of a
second cartesian coordinate system x and y. Here, the y-axis
is parallel to the radius vector transmitter-receiver and
coincides therefore with the propagation direction of the
wave passing the receiver. The x-y-system is rotated against the
X-Y-system in negative sense by the angle

$$\frac{\pi}{2} - \phi = \Psi_0 - \pi . \tag{1a}$$

The transformation is therefore

$$\begin{pmatrix} X \\ Y \end{pmatrix} = \begin{pmatrix} \cos(\Psi_0 - \pi) & \sin(\Psi_0 - \pi) \\ -\sin(\Psi_0 - \pi) & \cos(\Psi_0 - \pi) \end{pmatrix} \cdot \begin{pmatrix} x \\ y \end{pmatrix} \tag{2}$$

As further simplification we assume the distance between the
transmitter and the receiver to be so large that the received
field may be described by a combination of plane waves pro-
ceeding in the direction of wave normals parallel to the y-z-
plane (z being the vertical coordinate). The ground conducti-
vity is assumed to be so large that tangential components of
the electric vector immediately above the ground may be
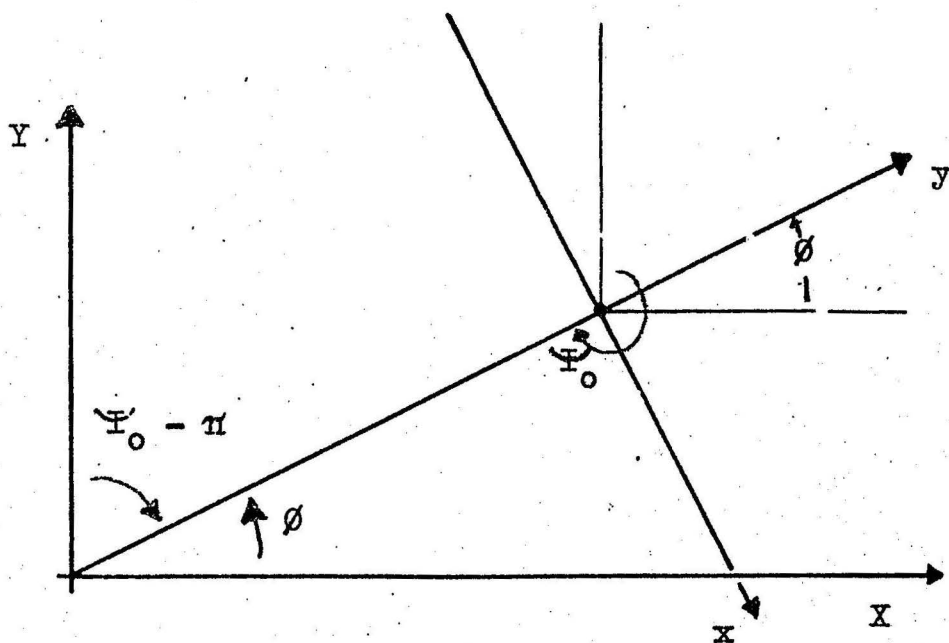neglected.

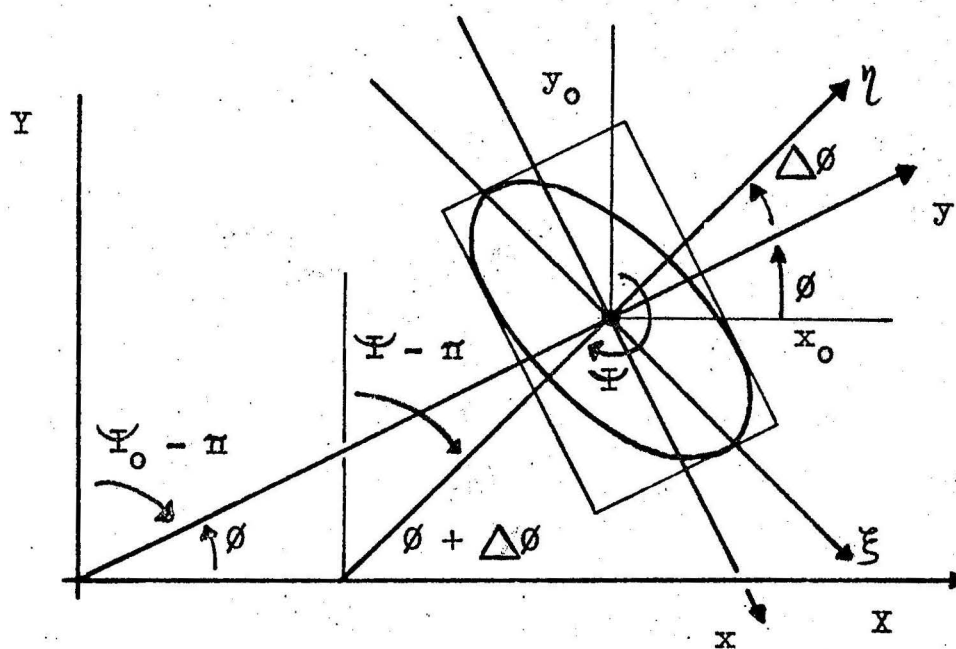Fig. 2: Configuration of the X-Y-system and the x-y-system

Fig. 3: H-oscillation ellipse and principal axes system

3.1 Transversal magnetic wave

Let us first consider the oversimplified case of a pure TM wave excited by a vertical dipole transmitter without any ionospheric reflection. Then the x-, y-, and z-directions coincide with the positive reference directions for the magnetic vector, the wave normal and the electric vector respectively.

The meaning of the coordinates X,Y, x and y will now be changed: In the following, X and Y symbolize the voltages excited by the magnetic vector in the X- and Y- loop antennas. Accordingly, x and y mean voltages that would be excited in loop antennas with normals in x- and y-direction. In the case of pure TM propagation we have (k_H = antenna constant):

$$x = k_H \frac{dH_x}{dt} \quad , \quad y = 0 \quad ,$$

$$X = k_H \frac{dH_X}{dt} = k_H \frac{dH_x}{dt} \cos(\Psi_0 - \pi) = -x \cos(\Psi_0) \quad (3)$$

$$Y = k_H \frac{dH_Y}{dt} = k_H \frac{dH_x}{dt} \sin(\Psi_0 - \pi) = x \sin(\Psi_0)$$

For deriving a voltage that indicates the direction Ψ_0, the voltage Y is phase shifted by 90° (the time dependence of all voltages is assumed to be $\exp(j\omega t)$). The phase shifted voltage jY is added to or subtracted from X to give the new voltages

$$U_I = X - jY = -x (\cos(\Psi_0) + j \sin(\Psi_0)) = -x \exp(+j\Psi_0)$$
$$(4)$$

$$U_{II} = X + jY = -x (\cos(\Psi_0) - j \sin(\Psi_0)) = -x \exp(-j\Psi_0)$$

The phase difference between U_I and U_{II} can easily be measured by a phase detector and is twice the bearing angle:

$$\frac{U_I}{U_{II}} = \exp(2 j \Psi_0) \quad (5)$$

In this way, the measurement of the bearing angle is reduced to a phase measurement appropriate for contineous observation.

3.2 Inclusion of a transversal electric field

The ionospheric reflection converts an incident TM wave partially to a TE wave. This leads to a horizontal component of the received magnetic vector parallel to the propagation direction. In a x-y-antenna system the following voltages would be induced:

$$x = k_H \frac{dH_x}{dt} \quad , \quad y = k_H \frac{dH_y}{dt} \quad\quad (6)$$

We may assume that the amplitude of y is mostly (but not generally) smaller than that of x, but the phase may vary arbitrarily. In the special case that the phase difference between y and x is 90°, the two voltages describe an ellipse, the larger principal axis coinciding with the x-axis. To this special case we relate the general case of an arbitrary phase difference δ writing as follows:

$$x = x_0\cos(\omega t), \quad\quad y = y_0\sin(\omega t + \delta) \quad\quad (7a)$$

or in complex form

$$\underline{x} = x_0\exp(j\omega t), \quad\quad \underline{y} = -jy_0\exp(j(\omega t + \delta)) \quad\quad (7b)$$

Both forms describe an ellipse the principal axes of which are rotated against the axes of the x-y-system by the "bearing error angle" $\triangle\phi$ (see Fig. 3).

In close analogy to equ. (7) we write the antenna voltages X and Y as follows

$$X = X_0\cos(\omega t + \delta_X), \quad Y = Y_0\sin(\omega t + \delta_Y) \quad\quad (8a)$$

or in complex form

$$\underline{X} = X_0\exp(j(\omega t + \delta_X)), \quad \underline{Y} = -jY_0\exp(j(\omega t + \delta_Y)) \quad\quad (8b)$$

The principal axes of the ellipse are rotated against the axes of the X-Y-system by the angle $\phi + \triangle\phi$, and it will be shown in the following that the "apparent bearing angle"

$$\Psi = \Psi_0 - \triangle\phi = (\tfrac{\pi}{2} - \phi - \triangle\phi) + \pi \quad\quad (9)$$

is indicated by our direction finding system.

The coordinates relative to the principal axis directions of the "H-oscillation ellipse" are ξ and η. Their physical significance is found analog to that of X, Y, x, and y described in the preceeding section. They obey the ellipse equation

$$\frac{\xi^2}{a^2} + \frac{\eta^2}{b^2} = 1 \tag{10}$$

where a and b are the larger and the smaller principal axis of the H-oscillation ellipse. In the ξ-η-system, the oscillation of the η-component is phase shifted against that of the ξ-component by 90°:

$$\xi = a\cos(\omega t + \delta_H), \qquad \eta = b\sin(\omega t + \delta_H) \tag{11a}$$

in complex form

$$\underline{\xi} = a\exp(j(\omega t + \delta_H)), \quad \underline{\eta} = -jb\exp(j(\omega t + \delta_H)) \tag{11b}$$

(Note that all phases are given here relative to that of the TM part of the magnetic vector!)

The larger axis a is always taken positive, the smaller axis b, however, may assume negative values. The sign of b describes the sense of the rotation of the magnetic vector.

The voltages excited by the ξ- and the η-component of the magnetic vector in the X- and the Y-antenna are found by a transformation analog to eq. (2):

$$\begin{pmatrix} X \\ Y \end{pmatrix} = \begin{pmatrix} \cos(\Psi - \pi) & \sin(\Psi - \pi) \\ -\sin(\Psi - \pi) & \cos(\Psi - \pi) \end{pmatrix} \begin{pmatrix} \xi \\ \eta \end{pmatrix} \tag{12a}$$

or in complex form, suppressing the time factor $\exp(j\omega t)$:

$$\begin{pmatrix} X_0\exp(j\delta_X) \\ -jY_0\exp(j\delta_Y) \end{pmatrix} = \begin{pmatrix} -\cos(\Psi) & -\sin(\Psi) \\ \sin(\Psi) & -\cos(\Psi) \end{pmatrix} \begin{pmatrix} a \\ b \end{pmatrix} \exp(j\delta_H) \tag{12b}$$

The voltages U_I and U_{II}, derived from X and the phase shifted voltage jY as in the preceeding section, are now (time factor suppressed):

$$\underline{U}_I = \underline{X} - j\,\underline{Y} = -(a - b)\,\exp(j(\Psi + \delta_H))$$

$$\underline{U}_{II} = \underline{X} + j\,\underline{Y} = -(a + b)\,\exp(j(-\Psi + \delta_H))$$
(13)

The phase difference is equal to twice the apparent bearing angle Ψ. By means of a phase detector it can easily be measured contineously. Furthermore, the amplitude of the ratio U_I/U_{II} which also is appropriate for being steadily recorded, is a unique function of the axis ratio b/a :

$$r_U = \frac{|U_I|}{|U_{II}|} = \frac{a - b}{a + b} = \frac{1 - b/a}{1 + b/a}$$
(14)

For a positive value of b, r_U is less than unity, for negative b it is greater . Thus, the sign of a logarithmic indication of r_U immediately allows to see the sense of rotation of the elliptically oscillating magnetic vector.

Finally, the larger axis a can be measured by rectifying the voltages U_I and U_{II} and adding:

$$|U_I| + |U_{II}| = 2a$$
(15)

If the positions of both, the transmitter and the receiver are given, then the true bearing angle Ψ_o is known and therefore the bearing error angle $\triangle\emptyset$ can be found from the apparent bearing angle Ψ (equ. 9). Therefore, the equations (13), (14), and (15) provide a complete determination of the parameters of the H-oscillation ellipse from the measured antenna voltages X and Y.

3.3 Relations between the ellipse parameters and the parameters of the TM and the TE field

3.3.1 Separation of the TM and TE component

The ellipse parameters a, b, and $\triangle\emptyset$ are given by the measurement. We want to determine the amplitudes x_o and y_o and the phase difference δ.

The principal axis system (ξ, η) is rotated against the x-y-system by the bearing error angle $\triangle\emptyset$. Substituting $\triangle\emptyset$ instead of ($\Psi - \pi$) in equ.(12a) and using the abbreviations

$$C = \cos(\triangle\emptyset) \quad , \quad S = \sin(\triangle\emptyset)$$

we get the transformation

$$\begin{pmatrix} x_o \\ -jy_o\exp(j\delta) \end{pmatrix} = \begin{pmatrix} C & -S \\ S & C \end{pmatrix} \cdot \begin{pmatrix} a \\ b \end{pmatrix} \exp(j\delta_H) \qquad (16)$$

In the same way as equ. (13) and (14) we find

$$\frac{\underline{x} - j\underline{y}}{\underline{x} + j\underline{y}} = \frac{x_o - y_o\exp(j\delta)}{x_o + y_o\exp(j\delta)} = \frac{1 - b/a}{1 + b/a} \exp(-2j\triangle\emptyset) \quad (17)$$

Equating the upper row of equ. (16) we find the relation between the phase δ_H and the ellipse parameters:

$$\delta_H = -\arctan(\tfrac{b}{a} \, tg(\triangle\emptyset)) \qquad (18)$$

The amplitudes x_o and y_o are related to a and b by

$$x_o^2 = \underline{x}\,\underline{x}^* = C^2a^2 + S^2b^2 \quad , \quad y_o^2 = \underline{y}\,\underline{y}^* = S^2a^2 + C^2b^2 \quad (19)$$

From here

$$x_o^2 + y_o^2 = a^2 + b^2 \qquad (20)$$

The phase difference δ can be found by adding and subtracting the following products:

$$\underline{x}\,\underline{y}^* = j\,x_oy_o\exp(-j\delta) = (a^2 - b^2)\,C\,S + j\,a\,b$$

$$\underline{x}^*\underline{y} = -j\,x_oy_o\exp(j\delta) = (a^2 - b^2)\,C\,S - j\,a\,b$$

$$\underline{x}\,\underline{y}^* + \underline{x}^*\underline{y} = -2\,x_oy_o\sin(\delta) = 2\,(a^2 - b^2)\,C\,S \qquad (21)$$

$$\underline{x}\,\underline{y}^* - \underline{x}^*\underline{y} = j2\,x_oy_o\cos(\delta) = j\,2\,a\,b \qquad (22)$$

Remembering that $C\,S = \frac{1}{2}\sin(2\triangle\emptyset)$ we find

$$\tan(\delta) = -\frac{(a^2 - b^2)}{2\,a\,b}\sin(2\triangle\emptyset) \tag{23}$$

The equations (20) and (22) form a set of equations for two unknown of the type:

$$u_1 + u_2 = p \;,\; u_1 u_2 = q \tag{24a}$$

with the solution

$$u_{1,2} = \frac{p}{2} \pm \sqrt{\frac{p^2}{4} - q} \tag{24b}$$

Inserting

$$p = a^2 + b^2, \quad q = \frac{a^2 b^2}{\cos^2(\delta)} = (a^2 b^2)(1 + \tan^2(\delta))$$

$$= a^2 b^2 + \frac{1}{4}(a^2 - b^2)^2 \sin^2(2\triangle\emptyset)$$

leads to

$$\left.\begin{array}{c} x_0^2 \\ y_0^2 \end{array}\right\} = \frac{a^2 + b^2}{2} \pm \frac{a^2 - b^2}{2}\sqrt{1 - \sin^2(2\triangle\emptyset)} \tag{25}$$

3.3.2 Calculation of the ellipse parameters from given TM and TE components.

For the application of theoretical field computations it is interesting to predict the ellipticity and the bearing error angle from given x_0, y_0, and δ. To this end we start from the inverse transformation to equ. (16) :

$$\begin{pmatrix} \underline{\xi} \\ \underline{\eta} \end{pmatrix} = \begin{pmatrix} a \\ b \end{pmatrix}\exp(j\delta_H) = \begin{pmatrix} C & S \\ -S & C \end{pmatrix}\begin{pmatrix} x_0 \\ -jy_0\exp(j\delta) \end{pmatrix} \tag{26}$$

an add the products

$$\underline{\xi}\,\underline{\eta}^* = -(x_0^2 - y_0^2)\,C\,S + j\,x_0 y_0(C^2\exp(-j\delta) + S^2\exp(+j\delta))$$

$$\underline{\xi}^*\underline{\eta} = -(x_0^2 - y_0^2)\,C\,S - j\,x_0 y_0(C^2\exp(+j\delta) + S^2\exp(-j\delta))$$

Because on the other hand

$$\underline{\xi}\,\underline{\eta}^* = j\,a\,b \qquad , \qquad \underline{\xi}^*\underline{\eta} = -j\,a\,b$$

the sum of the products vanishes, and we find

$$-(x_0^2 - y_0^2)\,C\,S + x_0 y_0 \sin(\delta)\,(C^2 - S^2) = 0$$

inserting

$$2\,C\,S = \sin(2\triangle\emptyset) \quad , \quad C^2 - S^2 = \cos(2\triangle\emptyset)$$

leads to

$$\tan(2\triangle\emptyset) = \frac{2\,x_0 y_0}{x_0^2 - y_0^2}\,\sin(\delta) \tag{27}$$

For deriving a and b from x_0, y_0, and δ , we insert in (24)

$$p = x_0^2 + y_0^2 \;,\quad q = x_0^2 y_0^2 \cos^2(\delta) = x_0^2 y_0^2 (1 - \sin^2(\delta))$$

and find

$$\left.\begin{matrix} a^2 \\ b^2 \end{matrix}\right\} = \frac{x_0^2 + y_0^2}{2} \pm \frac{x_0^2 - y_0^2}{2} \sqrt{1 + \left(\frac{2x_0 y_0}{x_0^2 - y_0^2}\,\sin(\delta)\right)^2} \tag{28}$$

3.3.3 Mapping of contours of constant ellipticity and constant bearing error angle.

A first inspection of equ. (7) leads to roughly scetching $\triangle\emptyset$ and b/a as functions of δ by the following remarkable values of δ:

δ	$y_0/x_0 < 1$		$y_0/x_0 > 1$	
	$\triangle\emptyset$	b/a	$\triangle\emptyset$	b/a
$-\frac{\pi}{2}$	$-\arctan(y_0/x_0)$ ($> -45°$)	0	$-\arctan(y_0/x_0)$ ($< -45°$)	0
0	0	y_0/x_0	$\mp 90°$	x_0/y_0
$\frac{\pi}{2}$	$+\arctan(y_0/x_0)$ ($< 45°$)	0	$+\arctan(y_0/x_0)$ ($> 45°$)	0
π	0	$-y_0/x_0$	$\pm 90°$	$-x_0/y_0$

For $\delta = \pm \frac{\pi}{2}$, the ellipticity vanishes and the bearing error angle passes extreme values. If δ is in the interval between $-\frac{\pi}{2}$ and $+\frac{\pi}{2}$, the sense of rotation of the magnetic vector is positive, otherwise negative.

For $\delta = 0$ or π, the ellipticity passes extreme values, and $\triangle\emptyset$ vanishes, if y_0/x_0 is less than unity. If y_0/x_0 is greater than unity, however, $\triangle\emptyset$ changes discontineously between $+ 90^o$ and $- 90^o$ when δ passes 0 or π . For $0 < \delta < \pi$, the bearing error angle is positive, and negative for the remaining interval.

To survey the content of the equations (23), (25), (27), and (28), the transformation between the ellipticity parameters and the complex TM-TE-ratio is graphically presented by figure 4. Here, contours of constant values of the observed parameters

$$\triangle\emptyset \text{ (in degrees) and } r_U = \frac{1 - \frac{b}{a}}{1 + \frac{b}{a}} \quad \text{(in dB)}$$

have been plotted on a plane defined by the following axes:

abscissa = phase difference δ between the TE and the
   TM component of the magnetic vector,
ordinate = ratio y_0/x_0 between the amplitudes of the
   two components (in dB).

For calculating contours of constant r_U, we start from the equations (20) and (22) and combine them to

$$\frac{\frac{b}{a}}{1 + \frac{b^2}{a^2}} = \frac{\frac{y_0}{x_0}}{1 + \frac{y_0^2}{x_0^2}} \cos(\delta) \qquad (29)$$

The left hand side of this equation can be expressed by the measured ratio r_U as follows:

$$\frac{b}{a} = \frac{1 - r_U}{1 + r_U} , \quad \frac{2\frac{b}{a}}{1 + \frac{b^2}{a^2}} = \frac{1 - r_U^2}{1 + r_U^2} = \ddot{v} \qquad (30)$$

Thus, lines of constant r_U are given by the solution of equ. (29):

$$\frac{y_o}{x_o} = \frac{\cos(\delta)}{v} \pm \sqrt{\frac{\cos^2(\delta)}{v^2} - 1} \qquad (31)$$

This solution is real in the range

$-90° < -\arccos(v) \leq \delta \leq +\arccos(v) < +90°$, when $r_U < 1$ and $v > 0$,

$90° < \arccos(v) \leq \delta \leq 2\pi - \arccos(v) < 270°$, when $r_U > 1$, $v < 0$.

The contours of constant $\triangle\emptyset$ are found from equ. (27), rewritten here as

$$\tan(2\triangle\emptyset) = u = \frac{2\frac{y_o}{x_o}}{1 - \frac{y_o^2}{x_o^2}} \sin(\delta) \qquad (27)$$

The solution is

$$\frac{y_o}{x_o} = -\frac{\sin(\delta)}{u} \pm \sqrt{\frac{\sin^2(\delta)}{u^2} + 1} \qquad (32)$$

To enshure that the solution is positive, the upper sign of the root has to be chosen. Because of the ambiguity of $\tan(2\triangle\emptyset)$, each contour corresponds to two values of $\triangle\emptyset$. For $y_o/x_o < 1$, $\triangle\emptyset$ is in the range between $-45°$ and $+45°$, for $y_o/x_o > 1$, $\triangle\emptyset$ is outside of this range. At the branch points $\delta = 0$ and $\delta = \pi$, each contour $\triangle\emptyset = $ const connects smoothly to a corresponding section of the contour $(\triangle\emptyset + \pi/2) = $ const or $(\triangle\emptyset - \pi/2) = $ const respectively.

$20 \log(r_U) = $

− 1	1
− 2	2
− 3	3
− 4	4
− 5	5
− 6	6
− 9	9
−12	12
−15	15
−18	18
−21	21
dB −24	24

30 —
20 —
10 —
0 —
-10 —
-20 —
↑ $\frac{y_o}{x_o}$
-30 —

$\delta = $ −90°   0°   90°   180°   270°

$\triangle\emptyset = $

−85	85	−85°
−80	80	−80°
−75	75	−75°
−70	70	−70°
•••	•••	•••
•••	•••	•••
−20	20	−20°
−15	15	−15°
−10	10	−10°
− 5	5	− 5°
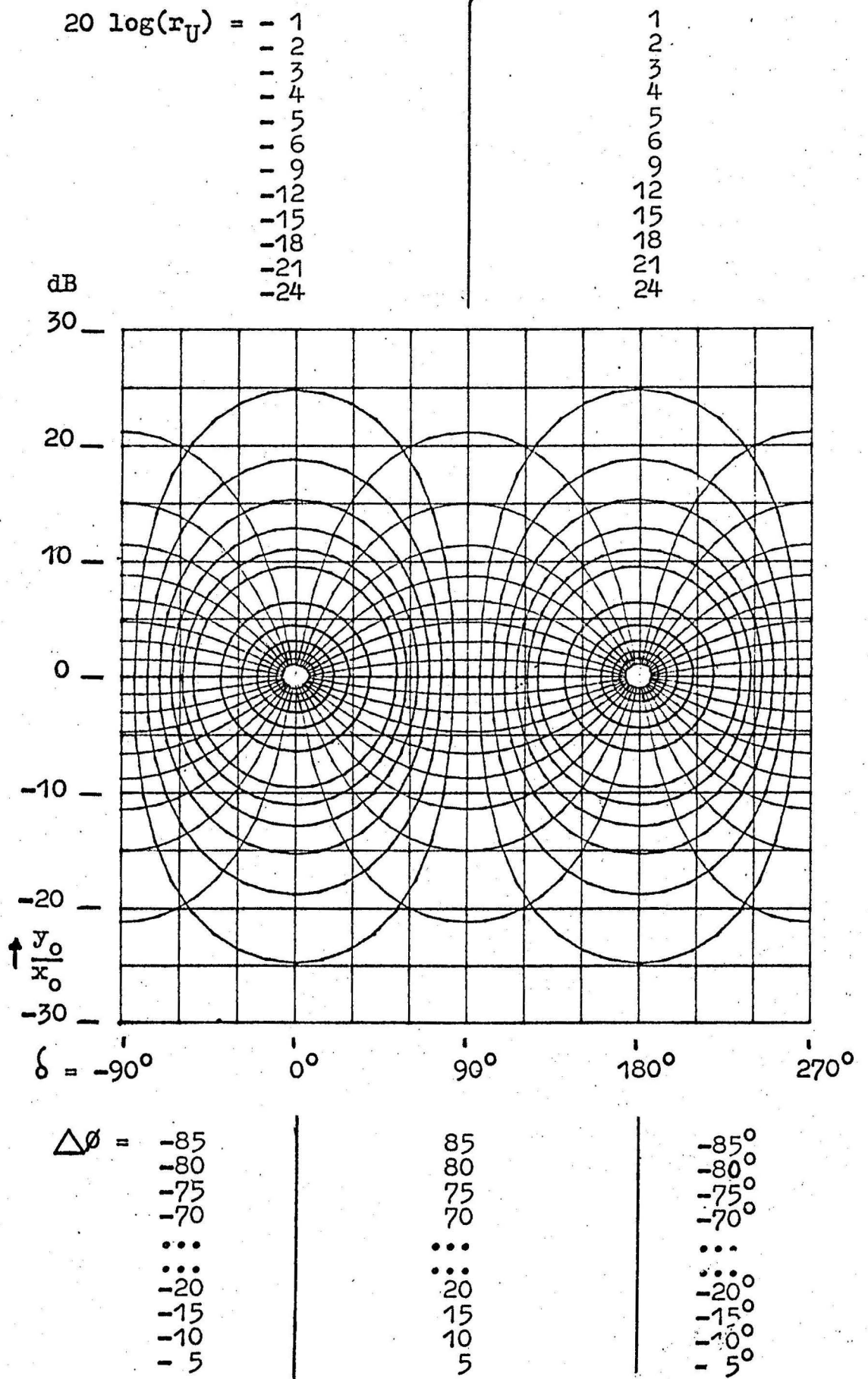
Fig. 4: Map of contours of constant r_U and constant $\triangle\emptyset$ in the $y_o/x_o - \delta -$ plane.

4. Examples of monthly observation reviews

The following pages show examples of monthly observation reviews that are planned to be communicated regularly for a limited period of two or three years, say. At the bottom of each page, the frequency and the observed parameter are indicated. For the graphical presentation, a format has been chosen that enables to visualize the influence of the sun's zenith angle on the observed parameters. To this end, strip chart records are carried out with small time resolution (2 cm/hr) and low indicating sensitivity for the observed quantities. These records can be combined without tim consuming copy work to monthly surveys. For more detailed studies of single events of special interest, synchronous records with higher sensitivity and time resolution (6 cm/hr) are available.

4.1 Individual time scale

For studying the sun's influence it is useful to superimpose upon the common GMT - time scale (horizontal in the presentation) an individual time scale for every propagation path and every day of the year. The propagation conditions for propagation paths of about 1000 km length, may approximately be defined by the state of the lower ionosphere above the path midpoint. The ionospheric ionization during the day is a function of the cosine of the sun's zenith angle χ. The individual time scale is therefore given by the instants when at the reference point $\cos(\chi)$ passes through the values 0.1, 0.2, ...and so on. The scale has been completed for the nighttime by the instants when $\cos(\chi)$ passes through the corresponding negative values. As an illustration we note that the $\cos(\chi)$-values -0.1 and -0.2 correspond to heights of the geometrical shadow above the ground of about 30 and 125 km respectively.

Berlin-HHI   MAR. 1971
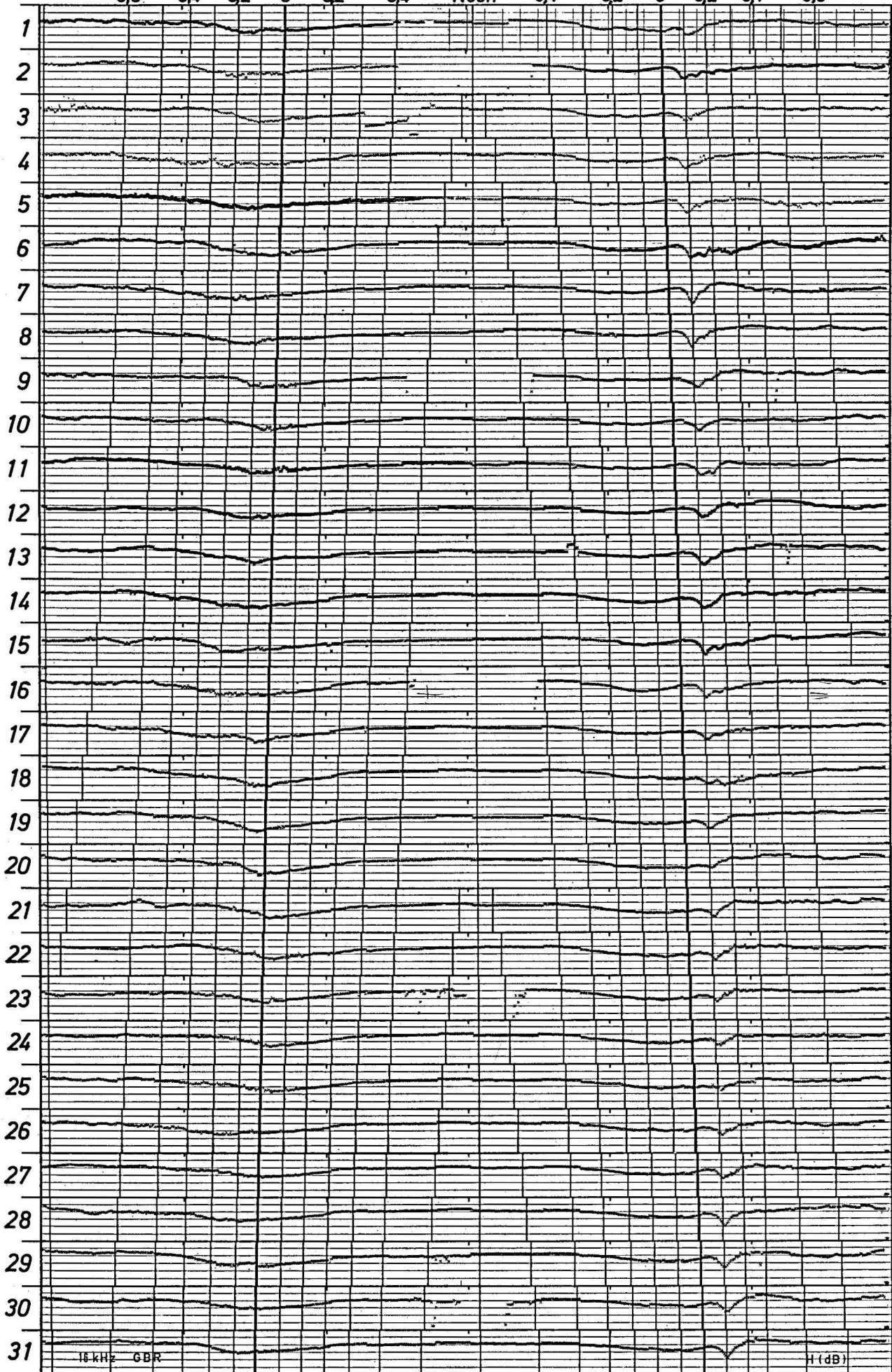
16 kHz GBR   H (dB)

Berlin - HHI   MAR. 1971
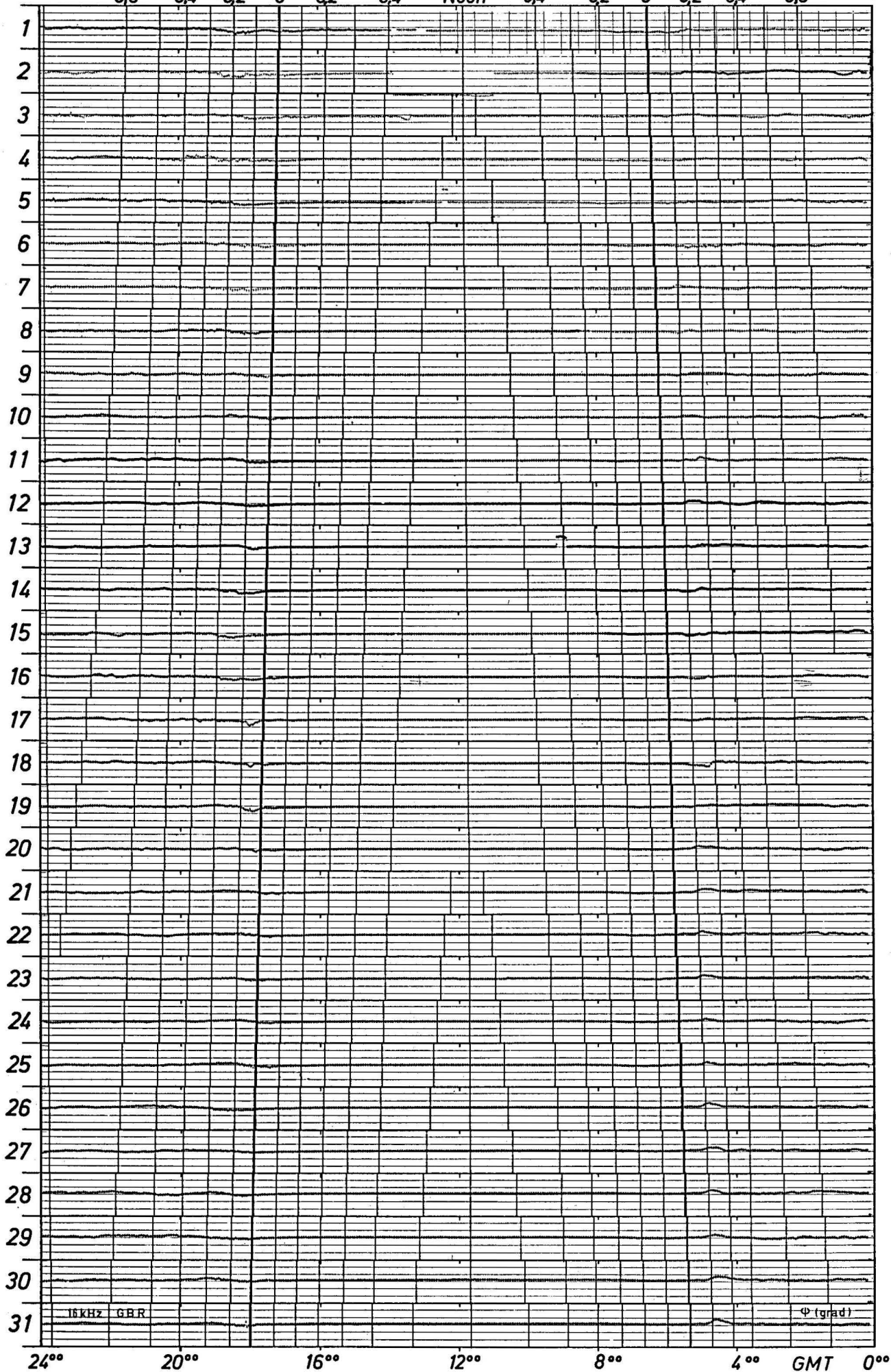
16 kHz GBR

φ (grad)

Berlin - HHI   MAR. 1971

Berlin - HHI   MAR. 1971

Frequency - Difference
Compensation not operating

16 kHz GBR

Φ_E (grad)
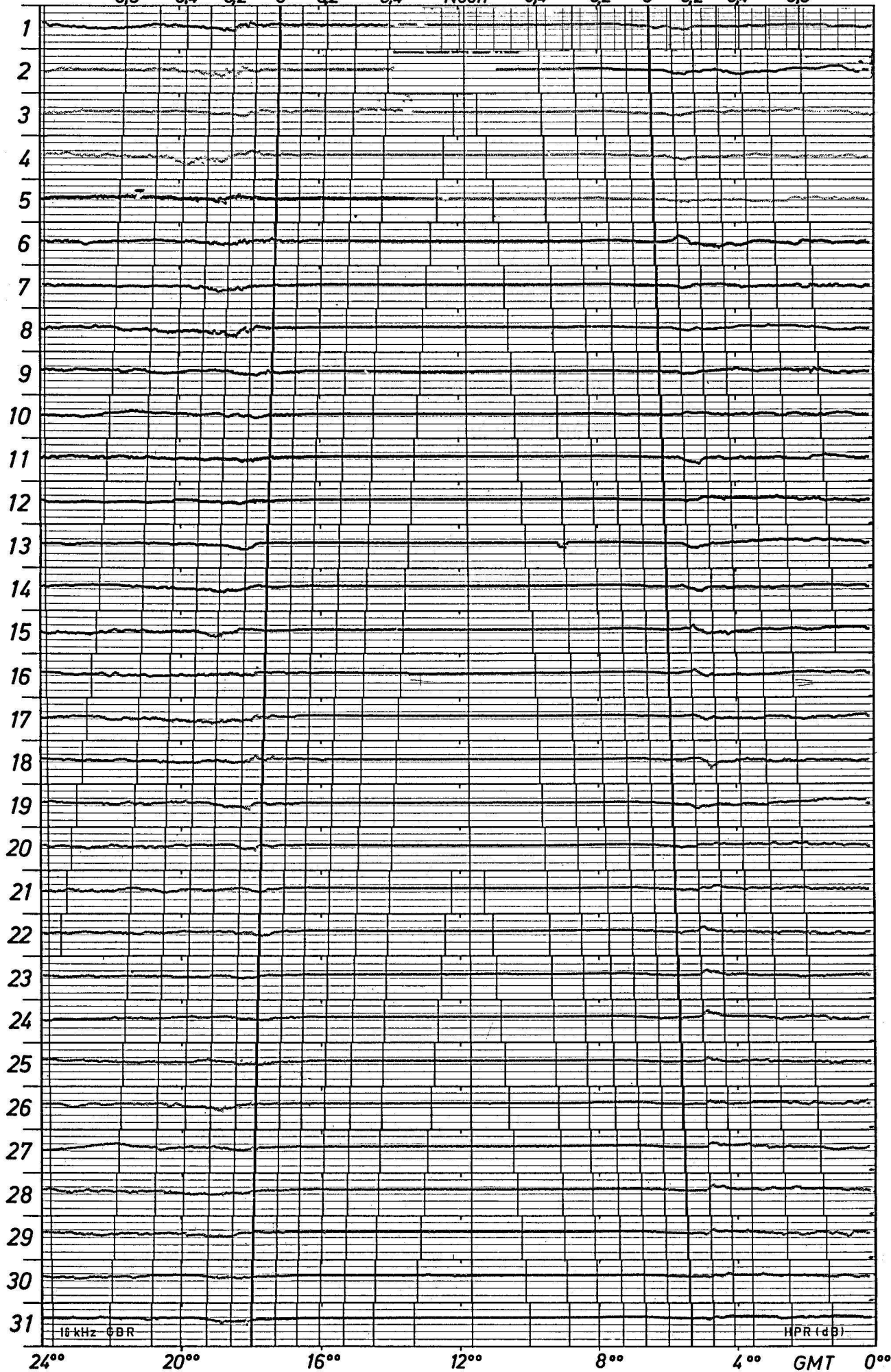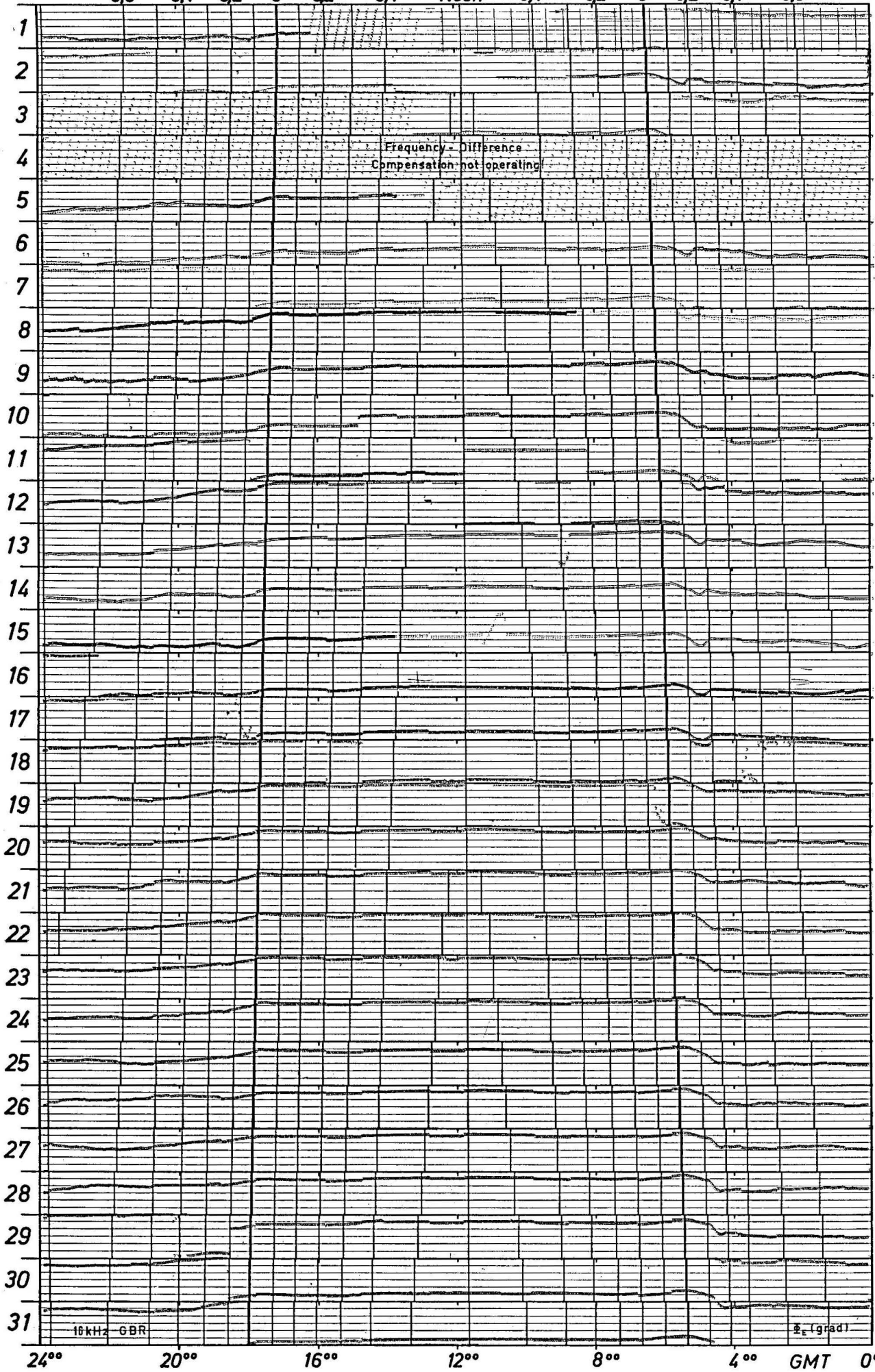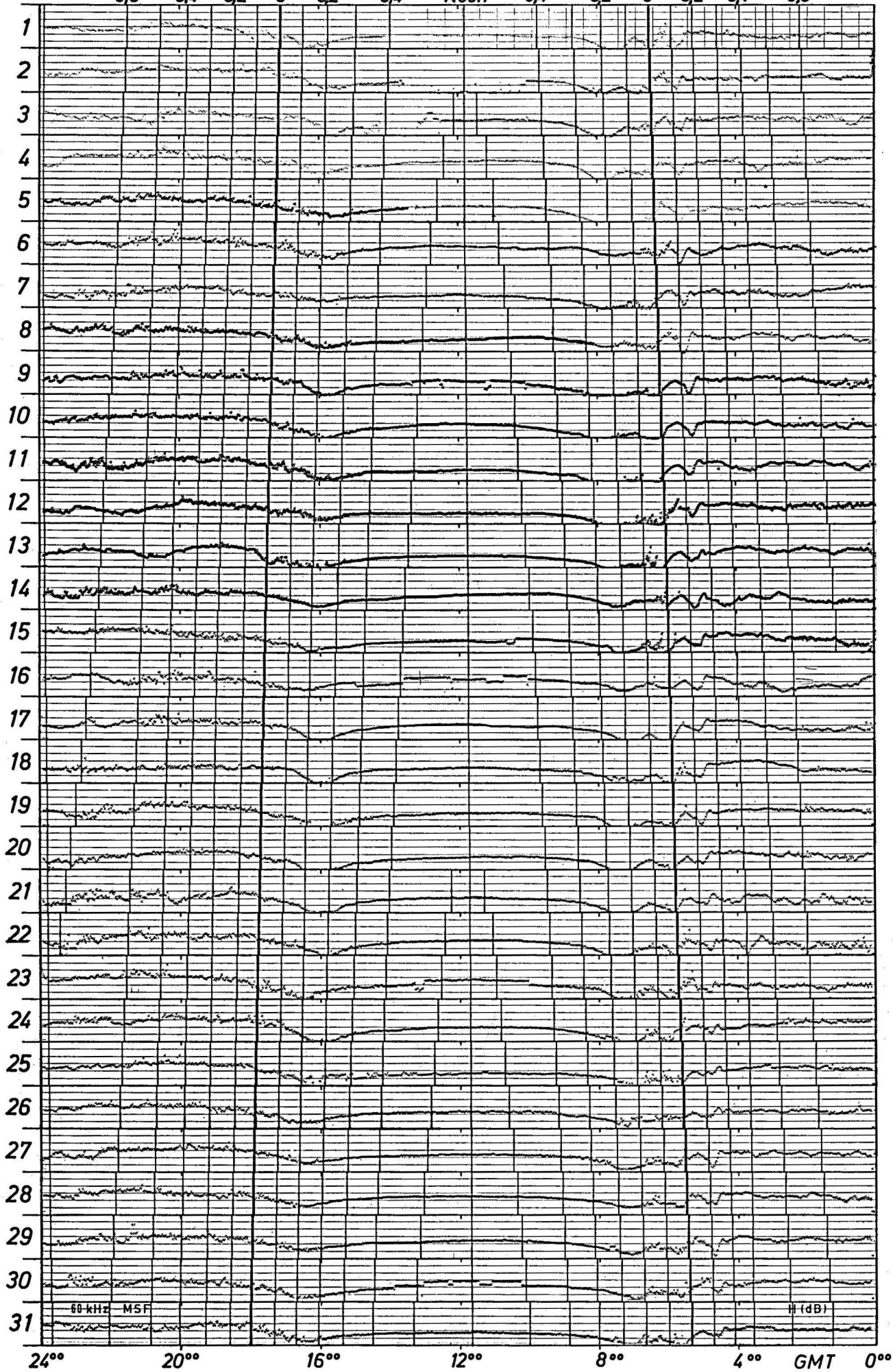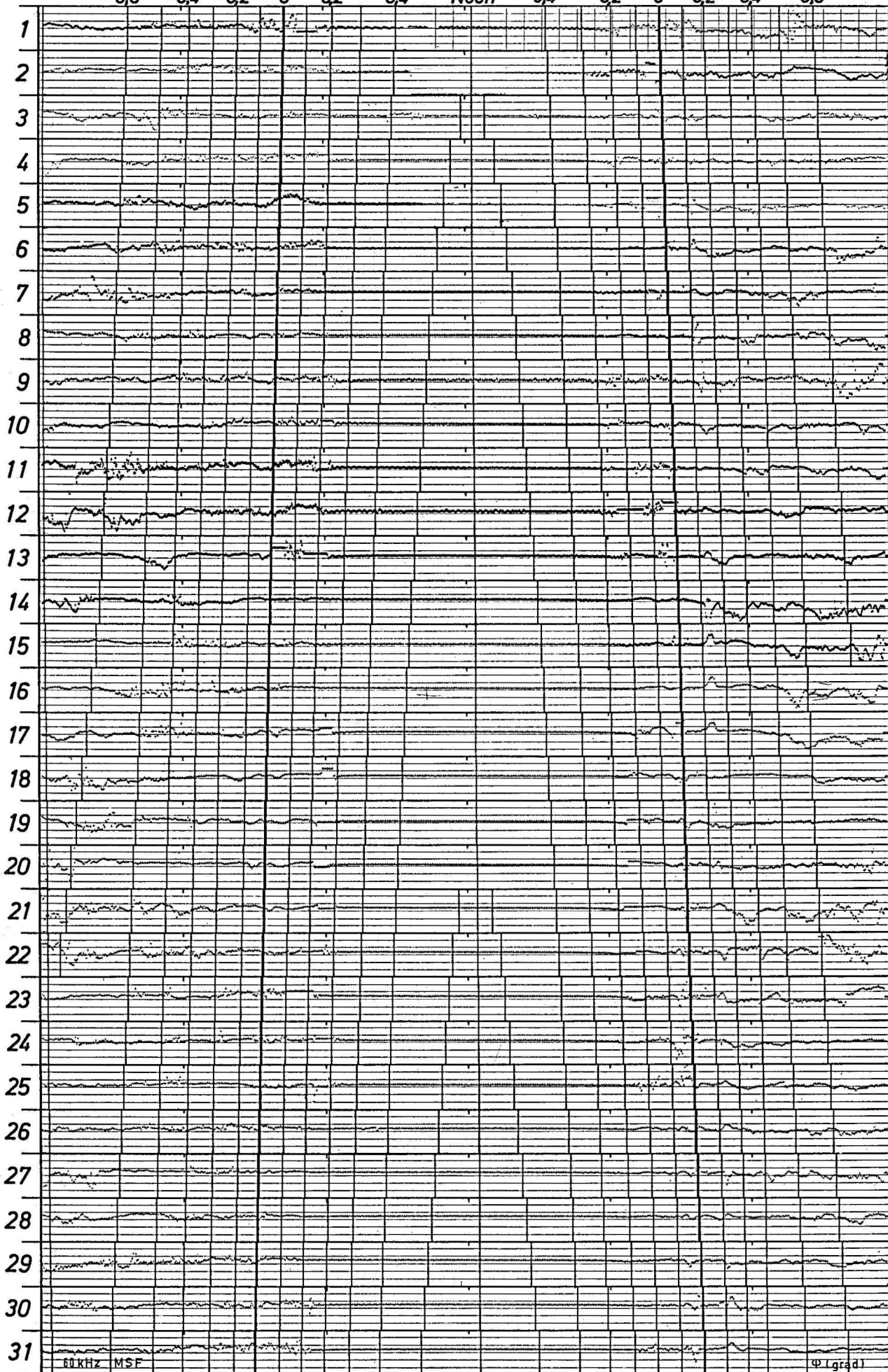
Berlin-HHI   MAR. 1971

60 kHz MSF   H (dB)

Berlin-HHI   MAR. 1971

60 kHz MSF   Φ (grad)

Berlin-HHI   MAR. 1971

60 kHz MSF   HPR (dB)
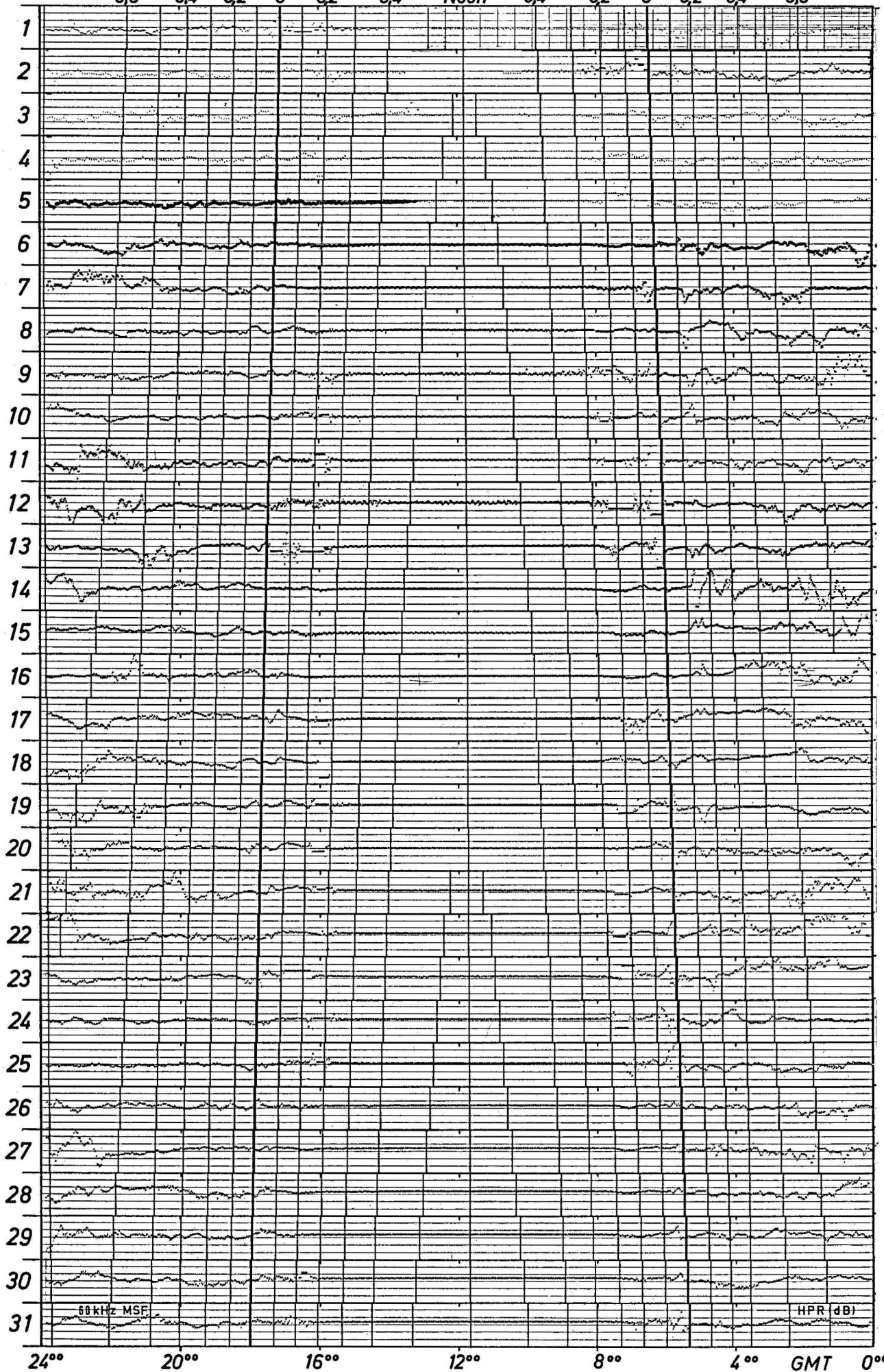
4.2 Indication scales

The amplitude H (relative to an arbitrarily chosen normal level) and the ratio HPR are given in dB. The indication range between the basic lines for the records of subsequent days corresponds to 36 dB.

The direction of arrival φ (identical to the $\triangle \emptyset$ of the text) and the phase $\bar{\Phi}_E$ are given in degrees. The indication range is 360° for Φ_E and 180° for φ.

The indication ranges are subdivided in 6 intervals corresponding to 6 dB, 30° or 60° respectively, and marked by tenuous horizontal lines in the presentation. The zero line for HPR and for φ is in the middle of the indication range. A positive deflection of the φ-track indicates a deviation of the apparent angle of arrival towards south.

5. Concluding remark

It should finally be mentioned that further development is planned to replace the graphical presentation with sets of numerical data appropriate for data exchange and automatic processing. It is believed that considerable reductions of the data abundance can be achieved without loss of essential information - at least for undisturbed days - when the observations are restricted to average quantities computed for the time intervals between the characteristic instants of the individual time scale. This hypothesis, however, needs substantiation by experience.

References:

Eppen, F., Heydt, G.   1959   Eine Registrierempfangsanlage für Längstwellen

Techn. Bericht Nr. 35 des Heinrich-Hertz-Instituts für Schwingungsforschung, Berlin-Charlottenburg.

Frisius, J.   1966   On the Determination of VLF Propagation Parameters by Field strength Measurements over Medium Distances

Radio Science 1 (New Ser.), No. 513 - 522

Frisius, J.   1970   Observations of Diurnal Amplitude and Phase Variations on 16 kHz Transmission Path and Interpretation by a simple Propagation Model.

AGARD Conference Proceedings No. 33, "Phase and Frequency Instabilities in Electromagnetic Wave Propagation" (Ed.: K. Davies), Slough, pg. 77 - 85

Heydt, G.   1967   Peilanlagen zur Messung von spektralen Amplitudenverteilungen, Amplitudenverhältnissen und Gruppenlaufzeitdifferenzen

Techn. Bericht Nr. 90 des Heinrich-Hertz-Instituts für Schwingungsforschung, Berlin-Charlottenburg

Raupach, R.   1971   Elektronischer Frequenzfehler-Kompensator zur Korrektur von Frequenzablagen zwischen $4 \cdot 10^{-8}$ und $2,5 \cdot 10^{-10}$.

Technischer Bericht Nr. 134 des Heinrich-Hertz-Instituts für Schwingungsforschung, Berlin-Charlottenburg

Raupach, R., Heydt, G.   1971   VLF Registrieranlage zur Messung von Einfallsrichtung, Polarisation, Phase und Amplitude von Sendersignalen.

Technischer Bericht Nr. 138 des Heinrich-Hertz-Instituts für Schwingungsforschung, Berlin-Charlottenburg

Volland, H.   1960   Zur Tagesausbreitung von Längstwellen über eine Entfernung von 1000 km

Techn. Bericht Nr. 37 des Heinrich-Hertz-Instituts für Schwingungsforschung, Berlin-Charlottenburg

Volland, H.   1968   Die Ausbreitung langer Wellen

Vieweg & Sohn, Braunschweig.